Applied Physics B (2022) 128:203
https://doi.org/10.1007/s00340-022-07922-8

Applied Physics B
Lasers and Optics

RESEARCH

Picosecond synchronously pumped diamond Raman laser

Shuanghong Ding[1] · Xinxin Huang[1] · Qiaoshuang Zou[1]

Received: 1 September 2022 / Accepted: 10 October 2022 / Published online: 15 October 2022

Abstract
With diamond crystals as Raman media, picosecond synchronously pumped solid-state Raman laser is theoretically studied in detail for the first time. High efficient working point and effective pulse compression working point are investigated. For both 532 nm and 1064 nm pumping, high Raman conversion efficiency can be achieved for negative cavity length detuning (Δx) and diamond crystal length of 5 mm. The higher efficiency can be obtained with longer Raman crystal, longer pumping pulse width and higher pumping power. For 532 nm pumping, effective pulse width compression can be realized for $\Delta x = 0$ nearby and diamond crystal length of 10 mm. Shorter pulse width and higher peak power of 1st Stokes laser can be achieved with longer Raman crystal, shorter pumping pulse width and higher pumping power. The findings can contribute to the design and optimization of picosecond synchronously pumped diamond Raman lasers.

1 Introduction

Diamond crystal has large hardness, high thermal conductivity and inactive chemical properties. Diamond crystals grown artificially with chemical vapor deposition (CVD) have very high purity and low stress birefringence. Due to excellent properties, diamond crystals have attracted much attention in recent years as Raman media [1–6]. The Raman gain of diamond is high, which is 12.5 cm/GW and 78 cm/GW at wavelengths of 1240 nm and 355 nm, respectively, and leads to very high SRS conversion efficiency. At the same time, the frequency of the main Raman mode of diamond crystals is 1332 cm^{-1}, and the large frequency shift can be produced. High efficient Raman conversions in ultraviolet, visible and infrared regime have been realized in diamond crystals [2–6]. In 2009, Mildren et al. used CVD single crystal diamond as the Raman medium, and achieved the SRS conversion efficiency of 63.5% with 532 nm pumping laser by adopting an external cavity structure [2].

The synchronously pumping way can enhance SRS conversion efficiency of ps pulses, where the time interval of adjacent pumping pulses is equal to the cavity round trip time of the extracavity Raman laser. In recent years, there are research reports on experiments of ps synchronously pumped solid-state Raman laser, and Stokes laser output of high conversion efficiency can be achieved. Furthermore, the effect of pulse width compression is observed experimentally, that is, the Stokes laser pulse width is much smaller than that of the pumping one. In 2010, Spence et al. adopted the 532 nm 26 ps pulsed laser as pumping source to simultaneously pump 6.7 mm long diamond crystal, and the pulse width was reduced to 9 ps [1].

The theoretical study of synchronously pumped solid-state Raman lasers can assist the design and optimization of lasers. In 2010, Granados et al. used transient coupled wave equations to conduct numerical simulation studies of synchronously pumped solid-state Raman lasers [7]. It was found that pulse compression comes from a combination of group velocity walk-off and strong pumping pulse depletion. In 2020, considering the spatial distribution of laser beams and phonon waves, our group deduced normalized SRS coupled wave equations in the transient state, and conducted numerical simulations of synchronously pumped solid-state Raman lasers [8]. Conditions of high Raman conversion and effective pulse width compression were explored numerically. It is concluded that higher dispersion or Raman gain leads to more intensive pulse width gain narrowing and intensity modulation, and favors pulse compression. In 2022, our group simulated output characteristics of synchronously pumped KGW Raman laser for pumping wavelength of 532 nm and 1064 nm by solving transient coupled wave equations [9].

✉ Shuanghong Ding
shding@ytu.edu.cn

[1] School of Physics and Electronic Information, Yantai University, Yantai 264005, China

There are research reports of ps synchronously pumped diamond Raman lasers, which have realized efficient Raman conversion, however effective pulse compression is not realized for ps pumping. With diamond crystals as the Raman media, more comprehensive and in-depth researches on ps synchronously pumped Raman lasers are needed. In this paper, transient coupled wave equations are adopted to numerically simulate output characteristics of ps synchronously pumped diamond Raman laser for pumping wavelength of 532 nm and 1064 nm. Results can contribute to the design and optimization of picosecond synchronously pumped diamond Raman lasers.

2 Theories

Nonlinear coupled wave equations describing the transient SRS interaction were deduced in detail [10]. In this paper, coupled wave equations in [7, 9] are adopted, which are derived under the reference frame moving with the group velocity of 1st Stokes laser v_s. Coupled wave equations and normalized form have been used to study properties of ps synchronously pumped Raman solid-state lasers [7–9].

Quantities adopted in the numerical analysis are defined as follows:

1. Intensity of 1st Stokes laser I_S (W/cm^2)

$$I_S = \frac{c\mu_S}{8\pi}|E_S|^2, \tag{1}$$

where E_S is of the electric field of 1st Stokes output, μ_S is the refractive index of 1st Stokes laser in Raman crystal, and c is the speed of light in vacuum.

2. Peak power of 1st Stokes laser $P_{S\,\max}$ (W)

$$P_{S\max} = A_S I_{S\max} = \frac{c\mu_S}{8\pi}A_S|E_{S\max}|^2, \tag{2}$$

where A_S is the cross-sectional area of 1st Stokes laser beam, $I_{S\,\max}$ is the peak intensity of 1st Stokes laser, and $E_{S\,\max}$ is the peak amplitude of 1st Stokes electric field.

3. Peak power ratio of 1st Stokes and pumping laser *Rpp*

$$Rpp = P_{S\max}/P_{\max}, \tag{3}$$

where $P_{\max}$ is the peak power of pumping pulse.

4. Pulse energy of 1st Stokes laser Φ_S (J)

$$\Phi_S = \frac{c\mu_S}{8\pi}A_S\int |E_S|^2 dt. \tag{4}$$

5. Conversion efficiency of 1st Stokes laser

$$\eta = \frac{\Phi_S}{\Phi_{L\,\mathrm{in}}}, \tag{5}$$

where $\Phi_{L\,\mathrm{in}}$ is the pulse energy of input pumping laser.

6. Pulse duration of 1st Stokes laser (ps)

$$\tau_S = \tau_{Sr} + \tau_{Sf}, \tag{6}$$

where τ_{Sr} is the rising time of I_S (0, t) from $I_{\mathrm{Smax}}/2$ to I_{Smax}, and τ_{Sf} is the falling time from I_{Smax} to $I_{\mathrm{Smax}}/2$.

3 Simulation conditions

A ring z-folded cavity configuration is utilized as illustrated in Fig. 1 [9], and the pumping and 1st Stokes laser propagate in the same direction inside the cavity. The cavity consists of four mirrors. M1 and M2 are curved mirrors having a beam waist radius of 33 μm (1/e^2 radius) at the diamond crystal. M1, M2 and M3 have coatings highly reflective at 1st Stokes wavelength, and highly transparent to fundamental and high-order Stokes lasers. The output coupler (OC) is highly transparent to high-order Stokes lasers, and has a reflectivity of R for 1st Stokes. All cavity losses are lumped in R of OC. The zero resonator length detuning Δx corresponds to 1st Stokes pulse being perfectly synchronized with the pumping pulse. For positive Δx, the cavity length of Raman laser is longer than that of zero detuning conditions. The round trip time of Raman laser is longer than the time interval of two adjacent pumping pulses, and 1st Stokes pulse will lag behind pumping pulse. For negative Δx, the Raman cavity length is shorter than that at zero detuning, and 1st Stokes pulse propagates ahead pumping pulse. The cavity length can be detuned by justifying M3.

Features of synchronously pumped diamond Raman lasers are investigated theoretically with transient nonlinear coupled wave equations for ps pumping sources of 532 nm and 1064 nm [9]. The interaction between 1st Stokes laser field circulating in the cavity and pumping pulse sequence is simulated until 1st Stokes pulse reaches a steady state. Cavity length detuning Δx is modeled by cyclically advancing or delaying 1st Stokes pulse after each round trip. Spatial distributions of the cavity mode is considered. λ_L, λ_S, G, L_r, T_2, R, P, t_p are the pumping laser wavelength, 1st Stokes wavelength, Raman gain, Raman crystal length, Raman mode dephasing time, output mirror reflectivity of 1st Stokes laser, pumping power and pumping pulse width, respectively. The SRS process of 1332 cm^{-1} Raman mode is researched for diamond crystals. Parameter values are listed in Table 1.

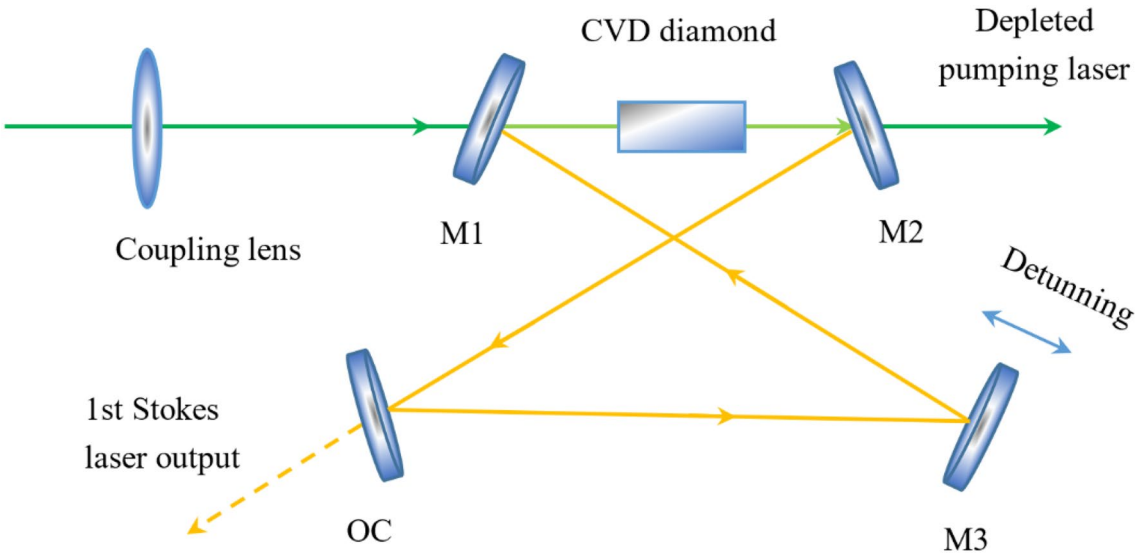

Fig. 1 Cavity setup of the synchronously pumped diamond Raman laser

Table 1 Parameters values

λ_L (nm)	λ_S (nm)	G (cm/GW)	L_r (cm)	P (W)	T_2 (ps)	R	t_p (ps)
532	573	50	0.5–3	1–7	6.8	0.7–0.95	5–30
1064	1240	12.5	0.67–3	1–7	6.8	0.88–0.90	10–26

4 Results and discussion

4.1 Output characteristics versus cavity length detuning

In 2010, Spence et al. used an Nd:YAG mode-locked laser with pulse repetition rate of 78 MHz and pulse width of 26 ps at 532 nm to synchronously pump diamond Raman laser, and achieved 1st Stokes laser output at 573 nm [1]. With experimental conditions in [1], the conversion efficiency, peak power ratio and pulse width of 1st Stokes laser are studied as a function of Δx as shown in Fig. 2 for $P = 7$ W, $t_p = 26$ ps, $L_r = 6.7$ mm and $R = 88\%$. Solid and dashed lines are for 532 nm and 1064 nm pumping, respectively. As shown in Fig. 2(a), as Δx increases, conversion efficiency of 1st Stokes laser keeps high value, then decreases rapidly after Δx is greater than − 25 μm. Conversion efficiency of 532 nm pumping is always greater than that of 1064 nm pumping. As shown in Fig. 2(b), for 1064 nm pumping, peak power ratio of 1st Stokes laser goes up slowly with the increase of Δx at the beginning, and then decreases rapidly after Δx is greater than − 12 μm. For 532 nm pumping, peak power ratio of 1st Stokes laser goes up slowly with the increase of Δx at the beginning, and then increases to maximum value of 1.2 around $\Delta x = 8$ μm, which is followed by a sudden declining. Peak power ratio of 532 nm pumping is always greater than that of 1064 nm pumping. The peak power of the input pumping pulse is 3.45×10^3 W.

The relationship between 1st Stokes pulse width and Δx is shown in Fig. 2(c). For both 532 nm and 1064 nm pumping, the pulse width decreases slowly with the increase of Δx at the initial stage, and drops sharply with Δx greater than − 25 μm. For 532 nm pumping, pulse width and conversion efficiency are 16.7 ps and 66.3% with $\Delta x = 8$ μm, and 7.7 ps and 28.5% with $\Delta x = 30$ μm. As Δx increases to 50 μm, the conversion efficiency drops to zero. Simulation results for 532 nm pumping are in good agreement with the experimental observations in [1]. However, it was found laser action ceases as Δx increases to + 200 μm in [1], which are + 50 μm in Fig. 2. This discrepancy arises from different definitions of zero cavity length detuning. In [1], $\Delta x = 0$ is defined as the cavity length of the lowest threshold of 1st Stokes laser, whereas, the zero resonator length detuning corresponds to perfect synchronization of 1st Stokes and pumping laser in this paper.

The Raman gain of diamond crystals is 50 cm/GW and 15 cm/GW at 532 nm and 1064 nm, respectively. Crystal length of 6.7 mm can achieve high-efficiency Raman conversion with negative Δx, and maximum conversion efficiency is 92% as shown in Fig. 2. In diamond crystals,

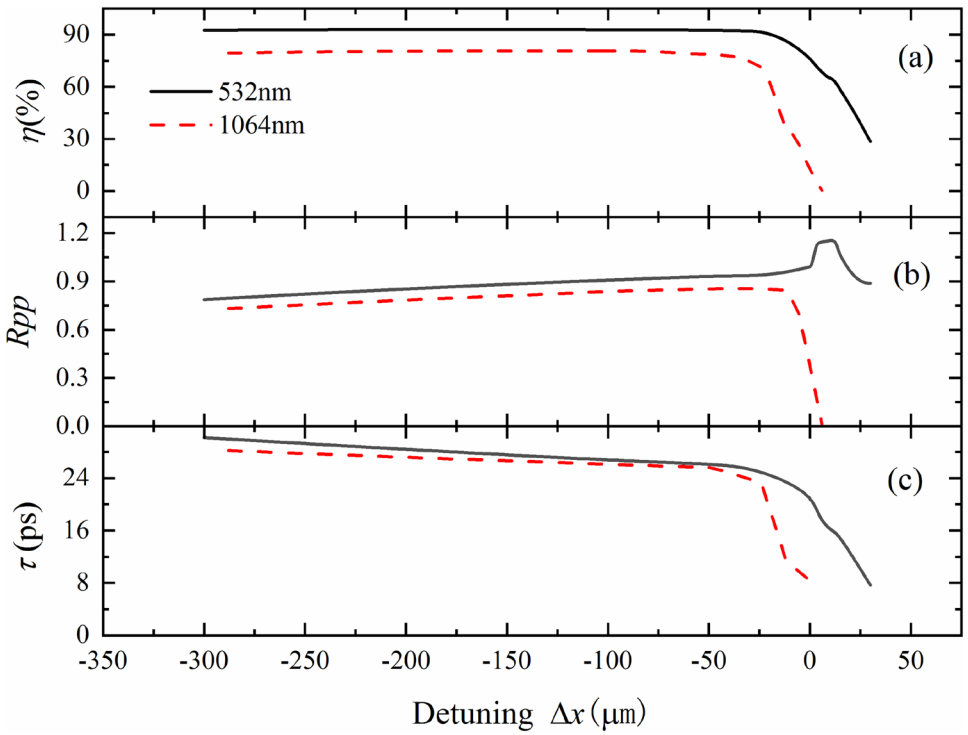

Fig. 2 With $P=7$ W, $t_p=26$ ps, $L_r=6.7$ mm and $R=88\%$, conversion efficiency (**a**), peak power ratio (**b**) and pulse width of 1st Stokes laser (**c**) are versus Δx. Solid and dashed lines are for 532 nm and 1064 nm pumping, respectively

the dispersion effect of the 532 nm is greater than that of the 1064 nm. With higher Raman gain and dispersion at 532 nm, more energy will be extracted from pumping pulse, and higher conversion efficiency and stronger pulse width compression effect can be obtained relative to 1064 nm pumping. However, due to the short crystal length, the maximum value of peak power ratio is 1.2, and smallest pulse width of 1st Stokes is 7.7 ps for 532 nm pumping. Thus, the effective pulse width compression is not accomplished. With narrower pumping pulse width and longer diamond crystal, the gain narrowing and intensity oscillation effects can be enhanced, which can bring about effect pulse width compression.

To further explore conditions for pulse width compression of ps synchronously pumped diamond Raman laser, longer diamond crystal and pumping laser of shorter pulse width are adopted in numerical simulation. In 2009, Granados et al. used a frequency doubled CW mode-locked Nd: YVO_4 laser at 532 nm as the pumping source, which had the average output power of 2 W, pulse width of 10 ps and pulse repetition rate of 80 MHz, and SRS conversion from 532 to 559 nm was realized in synchronously pumped KGW external cavity Raman laser [11]. With experimental conditions in [11], which are $R=88\%$, $P=2$ W and $t_p=10$ ps, the conversion efficiency, peak power ratio and pulse width of 1st Stokes laser are studied versus Δx for 532 nm pumping as shown in Fig. 3, where solid and dashed lines correspond to $L_r=30$ mm and $L_r=20$ mm, respectively.

As shown in Fig. 3(a), the conversion efficiency of $L_r=20$ mm is almost same as that of $L_r=30$ mm. As Δx increases, the conversion efficiency of 1st Stokes laser goes up very slowly to maximum value of about 92%, then decreases rapidly when $\Delta x>-6$ μm. As shown in Fig. 3(b), the peak power ratio increases slowly with Δx at the beginning, then increases rapidly when $\Delta x>-6$ μm. The highest peak power ratio of $L_r=30$ mm is 5.4 at $\Delta x=6$ μm, and that of 20 mm is 3.7 at $\Delta x=0$, which is followed by the sharp declining.

The relationship between 1st Stokes pulse width and Δx is shown in Fig. 3(c), which has a similar trend for both $L_r=20$ mm and $L_r=30$ mm. In the initial stage, the pulse width decreases slowly with Δx, and then drops sharply with Δx approaching 0, where the pulse compression effect occurs. Effective pulse width compression can be obtained, and the narrowest pulse width of 1st Stokes is 0.28 ps and 0.32 ps for $L_r=30$ mm and $L_r=20$ mm, respectively.

It is noted that synchronously pumped diamond Raman laser has two interesting working points for 532 nm pumping as shown in Fig. 3. One is high efficient working point with the negative detuning state of $\Delta x<-50$ μm, and the other is effective pulse compression working point with $\Delta x=0$ μm nearby, where high peak power and effective pulse width compression of 1st Stokes laser can be achieved.

For 1064 nm pumping, conversion efficiency, peak power ratio and pulse width of 1st Stokes laser are studied versus Δx for $R=88\%$ and $t_p=10$ ps as shown in Fig. 4, where solid lines correspond to $P=4$ W & $L_r=30$ mm,

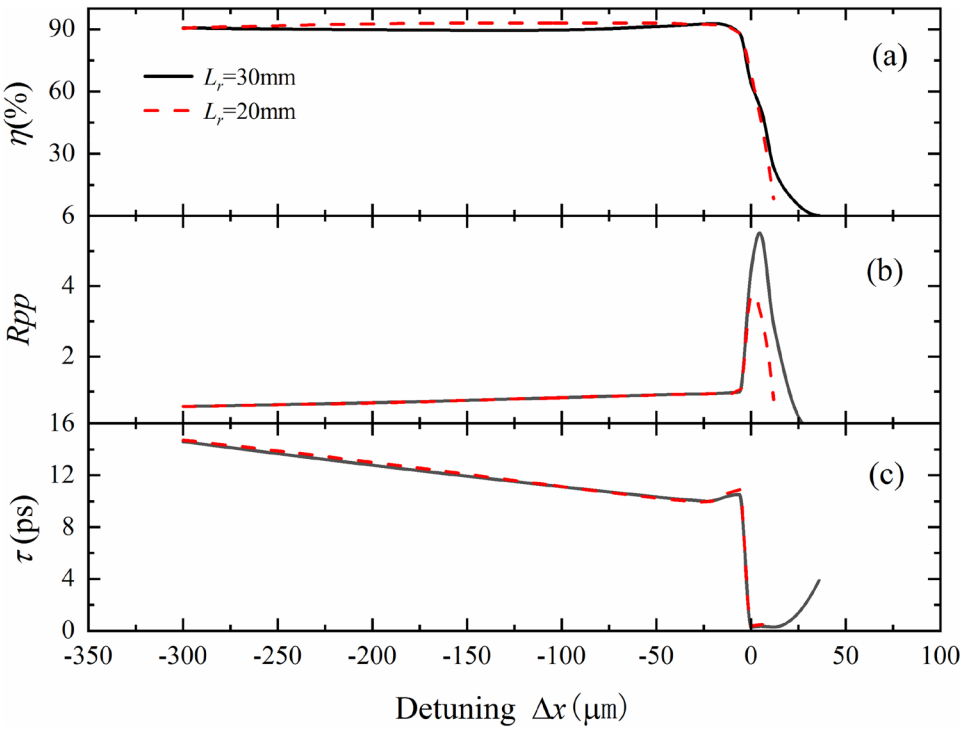

Fig. 3 With $R=88\%$, $P=2$ W and $t_p=10$ ps, conversion efficiency (**a**), peak power ratio (**b**) and pulse width (**c**) of 1st Stokes laser are versus Δx for 532 nm pumping. Solid and dashed lines correspond to $L_r=30$ mm and $L_r=20$ mm, respectively

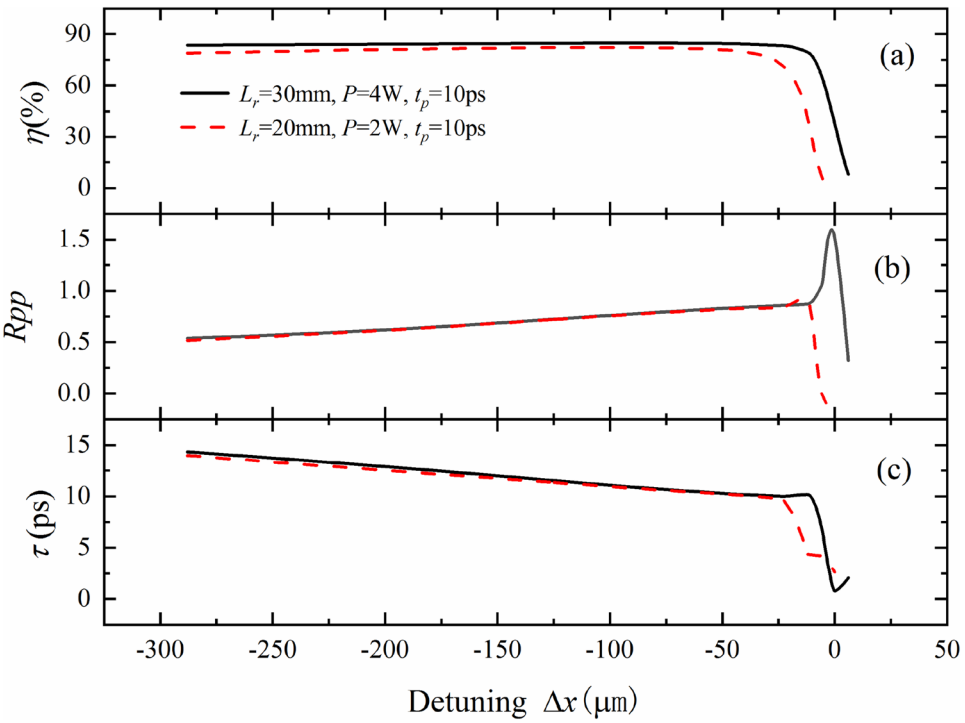

Fig. 4 With $R=88\%$ and $t_p=10$ ps, conversion efficiency (**a**), peak power ratio (**b**) and pulse width (**c**) of 1st Stokes laser is versus Δx for 1064 nm pumping. Solid lines correspond to $P=4$ W & $L_r=30$ mm, and dashed lines are for $P=2$ W & $L_r=20$ mm

and dashed lines are for $P=2$ W & $L_r=20$ mm. As shown in Fig. 4(a), as Δx increases, conversion efficiency of 1st Stokes laser goes up very slowly to maximum value, which is about 92% both for $P=4$ W & $L_r=30$ mm and $P=2$ W & $L_r=20$ mm, then decreases rapidly after Δx is greater than − 6 μm and − 50 μm for $P=4$ W & $L_r=30$ mm and $P=2$ W & $L_r=20$ mm, respectively. As shown in Fig. 4(b), peak power ratio increases slowly with the increase of Δx at the beginning. Then, peak power ratio increases rapidly to maximum value of 1.51 with

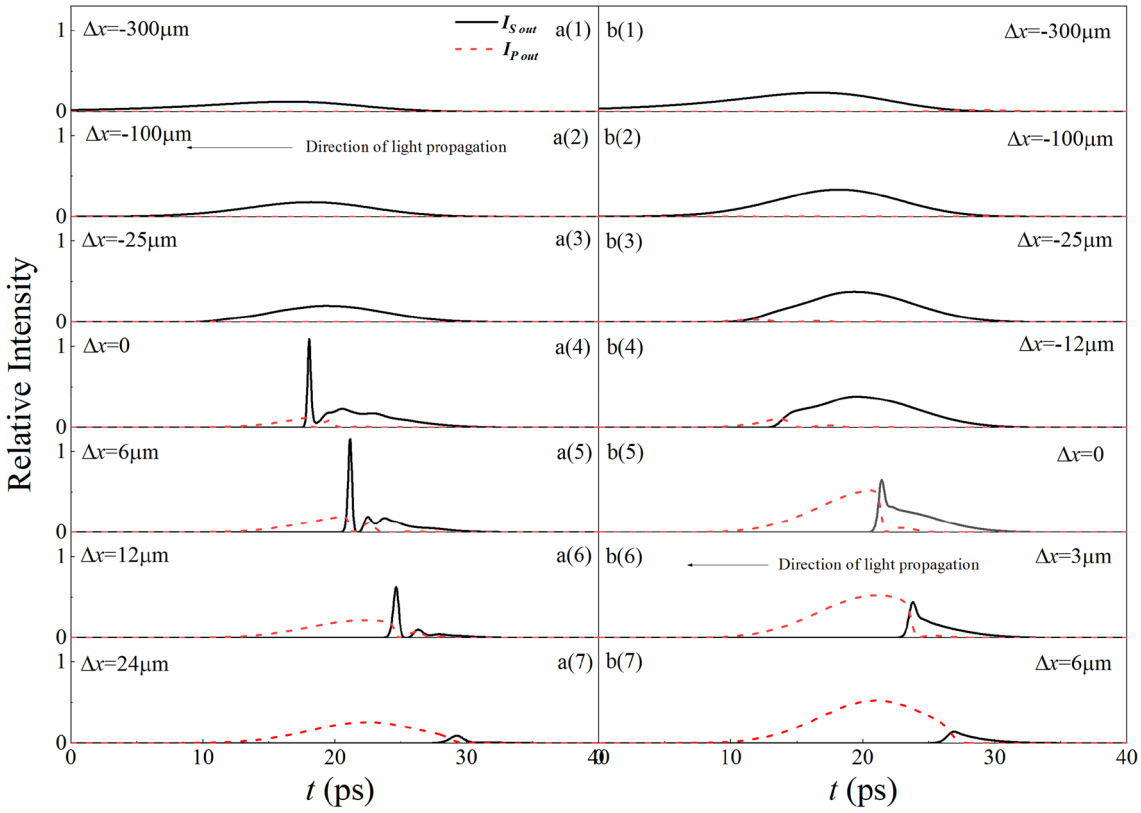

Fig. 5 For $R=88\%$, $L_r=30$ mm and $t_p=10$ ps, pulse waveforms of 1st Stokes output and depleted pumping laser are investigated versus Δx. For the pumping wavelength of 532 nm and $P=2$ W, pulse waveforms are shown in a(1)–a(7) with Δx of – 300 μm, – 100 μm, – 25 μm, 0 μm, 6 μm, 12 μm and 24 μm, respectively. For the pumping wavelength of 1064 nm and $P=4$ W, those are shown in b(1)–b(7) with Δx of – 300 μm, – 100 μm, – 25 μm, – 12 μm, 0 μm, 3 μm and 6 μm, respectively. Solid lines are pulse waveforms of 1st Stokes laser output, and dotted lines are those of depleted pumping laser. Laser travels from right to left with the reference system, as shown in a(2) and b(6)

$\Delta x=0$ for $P=4$ W & $L_r=30$ mm, and the maximum peak power ratio is 0.92 with $\Delta x=-15$ μm for $P=2$ W & $L_r=20$ mm. Peak power ratio of 1st Stokes laser decrease rapidly as Δx increases further for both conditions. 1st Stokes pulse width has a similar trend both for $P=4$ W & $L_r=30$ mm and $P=2$ W & $L_r=20$ mm as shown in Fig. 4(c). In the initial stage, the pulse width decreases slowly with the increase of Δx, and then drops sharply with Δx approaching − 6 μm and – 24 μm for $P=4$ W & $L_r=30$ mm and $P=2$ W & $L_r=20$ mm, respectively. For 1064 nm pumping, there is a slight pulse compression effect only for $P=4$ W & $L_r=30$ mm with $\Delta x=0$, where the maximum peak power ratio and minimum pulse width of 1st Stokes laser are 1.51 and 0.8 ps, respectively.

As shown in Figs. 2, 3 and 4, diamond crystal of very short length can achieve high-efficiency Raman conversion due to its high Raman gain for both 532 nm and 1064 nm pumping. However, effective pulse width compression can be realized with longer diamond crystal and pumping laser of shorter pulse width only for 532 nm pumping.

4.2 Pulse waveforms versus cavity length detuning

Pulse waveforms of 1st Stokes output and depleted pumping laser are illustrated versus Δx for $R=88\%$, $L_r=30$ mm and $t_p=10$ ps as shown in Fig. 5. Solid lines are pulse waveforms of 1st Stokes laser output, and dotted lines are those of depleted pumping laser. Laser travels from right to left with the reference system, as shown in Fig. 5a(2) and b(6). For pumping wavelength of 532 nm and $P=2$ W, pulse waveforms are shown in Fig. 5 a(1)–a(7) with Δx of – 300 μm, − 100 μm, − 25 μm, 0 μm, 6 μm, 12 μm and 24 μm, respectively. With negative Δx as shown in Fig. 5a(1)–a(3), there is no pulse compression effect, and pulse width and peak intensity of 1st Stokes laser are close to those of pumping laser pulses. In Fig. 5a(1) with $\Delta x=-300$ μm, 1st Stokes pulse has a long leading edge and a relatively steep trailing edge, and the pulse width is larger than that of the pumping pulse. At $\Delta x=-25$ μm, the pumping and 1st Stokes pulses in the Raman crystal overlap so well that pumping pulses are completely depleted as shown in Fig. 5a(3), and the highest Raman conversion efficiency is achieved. In Fig. 5a(4)–a(6),

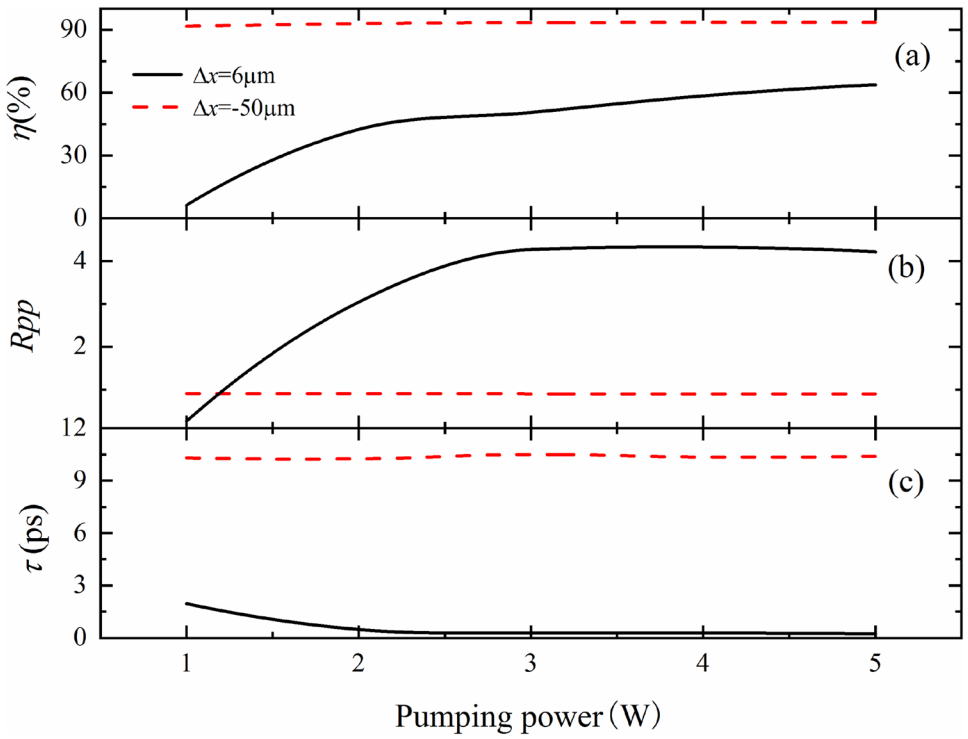

Fig. 6 Output characteristics of 532 nm synchronously pumped diamond Raman lasers are investigated versus pumping power under the conditions of $R=88\%$, $L_r=20$ mm and $t_p=10$ ps. Conversion efficiency (**a**), peak power ratio (**b**) and pulse width (**c**) of 1st Stokes laser is versus pumping power. Black solid lines correspond to $\Delta x=6$ μm, and red dashed lines are for $\Delta x=-50$ μm

$\Delta x=0,+6$ μm and $+12$ μm, respectively, pulse compression effect occurs, resulting in a shorter pulse width and greatly enhanced pulse peak power of 1st Stokes laser. The maximum peak intensity is obtained with $\Delta x=6$ μm as shown in Fig. 5a(5). Note that the group speed of pumping pulse is less than that of 1st Stokes pulse due to dispersion effect, and pumping pulses moves slowly to the right relative to the current frame. Under the condition of negative detuning, the dispersion effect has little effect on the SRS process. When there is zero detuning or positive detuning of small values, the leading edge of 1st Stokes pulse will sweep through the un-depleted part of the pumping pulse, and is amplified preferably. As a sequence, the leading edge of 1st Stokes pulse is steepened, and pulse width is compressed as shown in Fig. 5a(4)–a(6). As Δx increases to $+24$ μm, peak intensity and conversion efficiency of 1st Stokes laser decreases greatly as shown in Fig. 5a(7).

For the pumping wavelength of 1064 nm and $P=4$ W, pulse waveforms are shown in Fig. 5b(1)–b(7) with Δx of -300 μm, -100 μm, -25 μm, -12 μm, 0 μm, 3 μm and 6 μm, respectively. As shown in Fig. 5b(1)–b(4), pulse width and peak intensity of 1st Stokes laser are of the same order as those of pumping laser. In Fig. 5b(1), when $\Delta x=-300$ mm, 1st Stokes pulse has a long leading edge and steeper trailing edge, and the pulse width is larger than that of pumping laser pulse. For $\Delta x=-25$ μm as shown in Fig. 5b(3), the pump pulse is completely depleted resulting in high conversion efficiency. Although pumping power at 1064 nm is 4 W, which is two times of 532 nm pumping power, there is only a slight pulse compression effect with $\Delta x=0$ as shown in Fig. 5b(5). For $+3$ μm and $+6$ μm, as shown in Fig. 5b(6)–b(7), 1st Stokes pulse miss the peak of pumping one, and there is a reduction of Raman conversion.

As shown in Fig. 5, effective pulse compression effect and efficient Raman conversion can be realized for 532 nm pumping with diamond crystals, however, only efficient Raman conversion is available for 1064 nm pumping. In the following portion, 532 nm synchronously pumped diamond Raman lasers are investigated further.

4.3 Output characteristics versus pumping power

As shown in Fig. 6, under the conditions of $R=88\%$, $L_r=20$ mm and $t_p=10$ ps, conversion efficiency, peak power ratio and pulse width of 1st Stokes laser are investigated for different pumping powers. Black solid lines correspond to $\Delta x=6$ μm, and red dashed lines are for $\Delta x=-50$ μm. In Fig. 6(a), for high conversion efficiency working point with $\Delta x=-50$ μm, 1st Stokes laser conversion efficiency keep around 92% as pumping power increases from 1 to 5 W. For effective pulse compression working point with $\Delta x=6$ μm, the conversion efficiency rises monotonically with the increase of pumping power above the threshold of 1 W. When the pumping power is 5 W, the maximum conversion efficiency is 63.7%. As shown in Fig. 6(b), the peak power ratio goes up as the pumping power increases, then saturate when pumping power is higher than 3 W for $\Delta x=6$ μm. Whereas, the peak power ratio of $\Delta x=-50$ μm

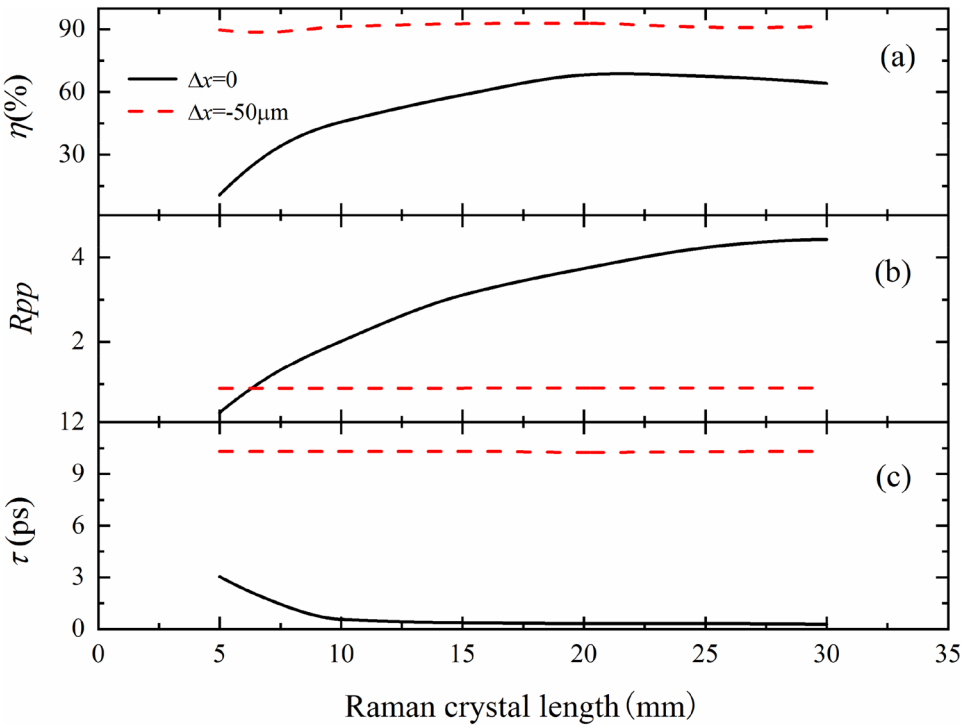

Fig. 7 Output characteristics of 532 nm synchronously pumped diamond Raman lasers are investigated versus Raman crystal length under the conditions of $R=88\%$, $P=2$ W and $tp=10$ ps. Conversion efficiency (**a**), peak power ratio (**b**) and pulse width (**c**) of 1st Stokes laser is versus Raman crystal length. Black solid lines correspond to $\Delta x=0$, and red dashed lines correspond to $\Delta x=-50$ μm

maintains at about 0.9. When the pumping power is 3 W, the peak power ratios are 4.27 and 0.90 for $\Delta x=6$ μm and $\Delta x=-50$ μm, respectively.

As shown in Fig. 6(c), the pulse width of 1st Stokes levels off at about 10.3 ps for $\Delta x=-50$ μm, and decreases significantly as pump powering increases for $\Delta x=6$ μm. When the pumping power is 5 W, the minimum pulse width is 0.24 ps for $\Delta x=6$ μm, which means effective pulse width compression.

Since diamond crystal has high Raman gain coefficient, pumping power has little effect on the performance of the high conversion efficiency working point. High pumping power will enhance the intensity modulation of 1st Stokes laser, which is beneficial for pulse width compression effect. High pumping power will improve the performance of pulse width compression, and realize 1st Stokes laser output of high conversion efficiency, high peak power and narrow pulse width. However, when pumping power is higher than 3 W, peak power ratio and pulse width of 1st Stokes laser tends to saturate, and performance cannot be enhanced by further increase of pumping power.

4.4 Output characteristics versus Raman crystal length

Under the conditions of $R=88\%$, $P=2$ W and $tp=10$ ps, conversion efficiency, peak power ratio and pulse width of 1st Stokes laser are studied with respect to Raman crystal length. Black solid lines correspond to $\Delta x=0$, and red dashed lines correspond to $\Delta x=-50$ μm, respectively. As shown in Fig. 7(a), with $\Delta x=-50$ μm, 1st Stokes laser conversion efficiency stays around 90% as Raman crystal length increases from 5 to 30 mm. With $\Delta x=0$, the conversion efficiency rises with Raman crystal length at first stage, then saturates when Raman crystal length is greater than 20 mm. The maximum conversion efficiency is about 68%. As shown in Fig. 7(b), the peak power ratio of $\Delta x=0$ goes up as Raman crystal length increases, and is much higher than that of $\Delta x=-50$ μm. When Raman crystal length is greater than 25 mm, the peak power ratio approaches the saturated value of 4.4. For $\Delta x=-50$ μm, the peak power ratio levels off at about 0.90 as the Raman crystal length increases.

As shown in Fig. 7(c), for $\Delta x=0$, pulse width of 1st Stokes laser rapidly declines as the crystal length increases from 5 to 10 mm. Effective pulse width compression can be achieved with Raman crystal greater than 10 mm. As Raman crystal length increases further, pulse width of 1st Stokes has no significant decrease. When the Raman crystal length is 30 mm, 1st Stokes pulse width is 0.28 ps for $\Delta x=0$. With $\Delta x=-50$ μm, the pulse width of 1st Stokes keeps about 10.3 ps.

Since diamond crystal has a high Raman gain coefficient, crystal of several millimeters can produce high conversion efficiency, so the length of the Raman crystal has little effect on the performance of the high conversion efficiency working point. Pulse width compression effects requires high Raman gain, on the other hand, its performance is highly

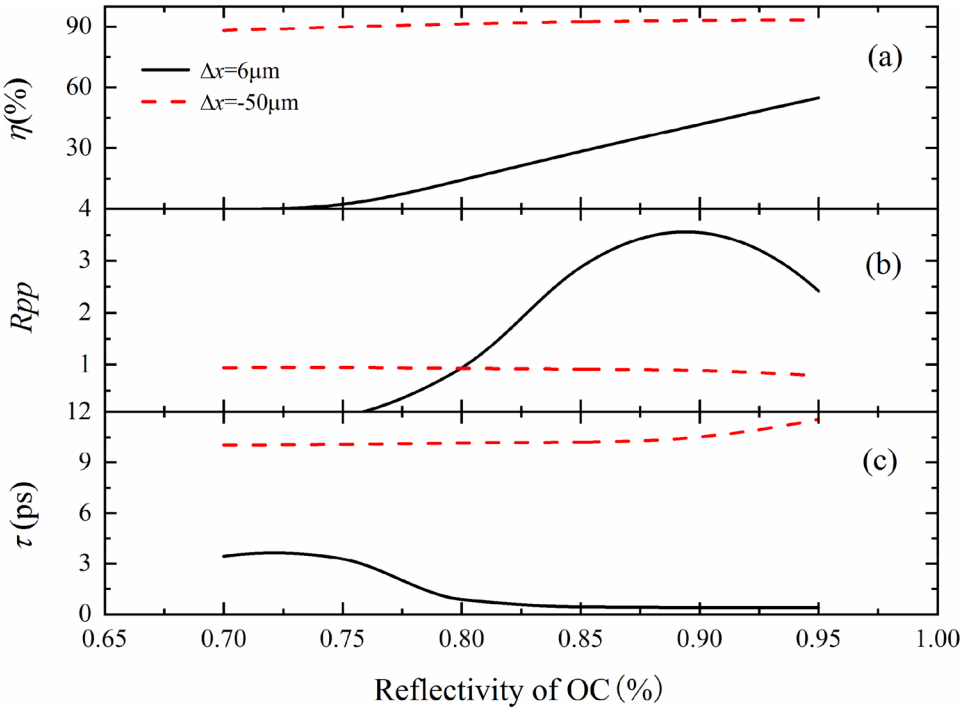

Fig. 8 Output characteristics of 532 nm synchronously pumped diamond Raman lasers are investigated versus OC reflectivity under the conditions of $L_r = 20$ mm, $P = 2$ W and $t_p = 10$ ps. Conversion efficiency (**a**), peak power ratio (**b**) and pulse width (**c**) of 1st Stokes laser is versus OC reflectivity. Black solid lines correspond to $\Delta x = 6$ μm, and red dashed lines correspond to $\Delta x = -50$ μm

dependent on the dispersion shift of 1st Stokes pulse relative to pumping pulse. A longer Raman crystal can achieve a larger dispersion shift, so the increase of Raman crystal length will improve the performance of the effective pulse width compression working point. However, as shown in Fig. 7, effective pulse width compression can be achieved with Raman crystal of 10 mm, and conversion efficiency and peak power ratio tend to be saturated with Raman crystal length of 20 and 25 mm, respectively. Since diamond crystals are so expensive, the length of 10–15 mm can achieve fairly good performance of pulse compression effect.

4.5 Output characteristics versus OC reflectivity

Under the conditions of $L_r = 20$ mm, $P = 2$ W and $t_p = 10$ ps, with Δx of − 50 μm and 6 μm, conversion efficiency, peak power ratio and pulse width of 1st Stokes laser versus OC reflectivity are studied. Black solid lines correspond to $\Delta x = 6$ μm, and red dashed lines correspond to $\Delta x = -50$ μm. As shown in Fig. 8(a), with $\Delta x = -50$ μm, 1st Stokes laser conversion efficiency increases slightly from 88 to 93% as reflectivity increases from 75 to 95%. For $\Delta x = 6$ μm, SRS threshold is reached for reflectance of around 75%, and then conversion efficiency increase monotonically with OC reflectivity to maximum value of 55%. As shown in Fig. 8(b), with $\Delta x = -50$ μm, the peak power ratio levels off at about 0.9 as the reflectivity increases. With $\Delta x = 6$ μm, the peak power ratio increases with reflectivity at first stage, and reaches the maximum value of 4.3 for the reflectivity of about 90%, which is followed by slow decrease with the further increase of reflectivity.

As shown in Fig. 8(c), with $\Delta x = -50$ μm, with the increase of the reflectivity of the output mirror, pulse width of 1st Stokes laser keep stable at 10 ps, then increases slowly. High OC reflectivity will increase the lifetime of 1st Stokes photon, and results in longer pulse width. With $\Delta x = 6$ μm, after 1st Stokes laser reaches the threshold, pulse width first slowly decreases with reflectivity, then remains stable.

OC reflectivity has little effect on the performance of the working point of high conversion efficiency. For $\Delta x = 6$ μm, conversion efficiency and peak power can be enhanced by increasing the reflectivity, however, so high reflectivity cannot further improve peak power. There is an optimum coupling output rate.

4.6 Output characteristics versus pumping pulse width

As shown in Fig. 9, under the conditions of $R = 88\%$, $L_r = 20$ mm and $P = 2$ W, keeping pumping pulse energy unchanged, for Δx of − 50 μm, 6 μm and 0, conversion efficiency, peak power ratio and pulse width ratio of 1st Stokes laser are researched versus pumping pulse width. Black solid, blue dotted and red dashed lines correspond to $\Delta x = 6$ μm, $\Delta x = -50$ μm and $\Delta x = 0$, respectively. As shown in Fig. 9(a), for $\Delta x = -50$ μm and 0, conversion efficiency of 1st Stokes laser remains almost unchanged with the increase of pumping pulse width, which are about 92% and 65%, respectively. For $\Delta x = 6$ μm, the conversion

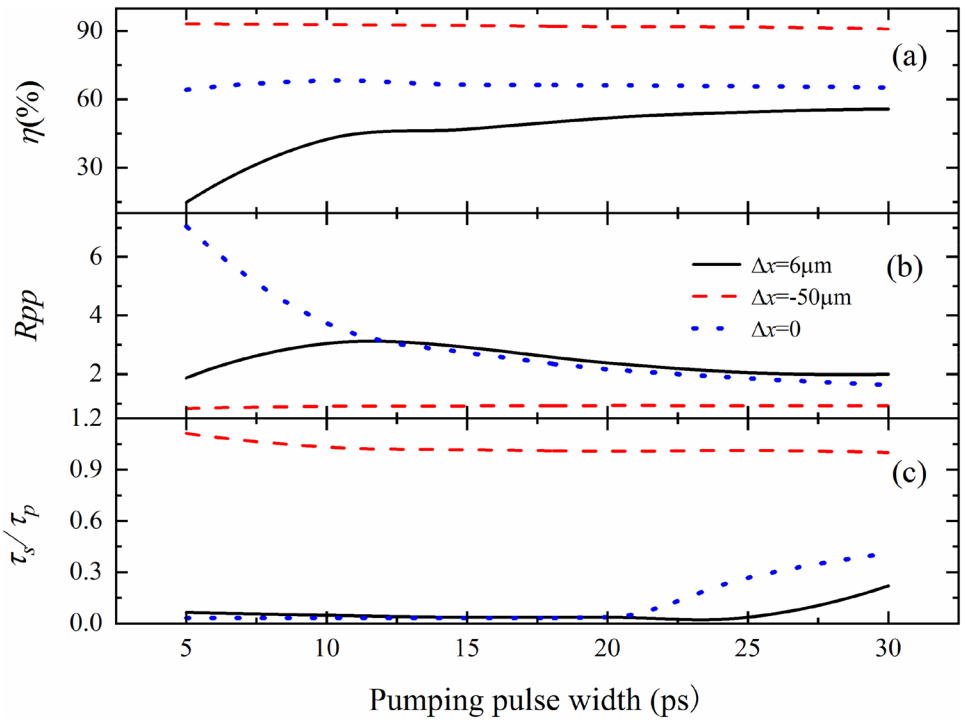

Fig. 9 Output characteristics of 532 nm synchronously pumped diamond Raman lasers are investigated versus pumping pulse width under the conditions of $R=88\%$, $L_r=20$ mm and $P=2$ W. Conversion efficiency (**a**), peak power ratio (**b**) and pulse width ratio (**c**) of 1st Stokes laser is versus pumping pulse width. Black solid, blue dotted and red dashed lines correspond to $\Delta x=6$ μm, $\Delta x=-50$ μm and $\Delta x=0$, respectively

efficiency significantly increases as pumping pulse width increase from 5 to 10 ps, then increases slowly with pumping pulse width.

With the reduction of pumping pulse width, the peak power of pumping pulse will increase for the same pumping pulse energy, thus the peak power ratio is more appropriate to illustrate output performance. As shown in Fig. 9(b), with $\Delta x=-50$ μm, peak power ratio keeps the value of about 1 as pumping pulse width increase from 5 to 30 ps. With $\Delta x=6$ μm, the peak power ratio increases to the maximum value of 3 as pumping pulse width increases from 5 to 10 ps, and then declines slightly as pumping pulse width further increase. For $\Delta x=0$, the peak power ratio has the maximum value of 7 with pumping pulse width of 5 ps, and decreases monotonically as pumping pulse width increases from 5 to 30 ps. For ps synchronously pumped Raman laser, pulse width compression can be achieved with zero or positive Δx. Raman laser can tolerance very smaller positive value of Δx, and conversation efficiency decreases rapidly to zero as Δx goes from negative value to positive value. There is an optimum value of Δx to achieve the highest peak power and smallest pulse width of 1st Stokes laser, which is highly related to pumping pulse width. The optimum value of Δx is zero for pumping pulse width of 10 ps, and is 6 μm for pumping pulse width of 20 ps. Greater positive value of Δx can be tolerated for larger pumping pulse width.

As shown in Fig. 9(c), with $\Delta x=-50$ μm, there is no obvious pulse width compression phenomenon, and pulse width of 1st Stokes laser is approximately equal to the pulse width of the pumping laser. For example, when the pump pulse width is 5 ps, the pulse width of 1st Stokes light is about 5.6 ps. Pulse width of 1st Stokes laser is effectively compressed with pumping pulse width less than 20 ps and 25 ps for $\Delta x=0$ μm and 6 μm, respectively.

5 Conclusion

In this paper, synchronously pumped solid-state diamond Raman laser is theoretically studied based on the Raman mode of 1332 cm^{-1} by numerically solving transient nonlinear coupling equations. Raman output characteristics for the pumping wavelength of 532 nm and 1064 nm are researched versus cavity length detuning. It is found that high efficiency Raman conversion can be achieved with diamond crystal of several millimeter for both 532 nm and 1064 nm pumping due to its very high Raman gain. The dispersion and Raman gain at 532 nm are greater than those at 1064 nm, and effective pulse width compression can be realized for 532 nm pumping.

532 nm synchronously pumped diamond Raman lasers are investigated in detail. It is noted that synchronously pumped diamond Raman laser has two interesting working points for 532 nm pumping. One is high conversion efficiency working point with the negative detuning state of $\Delta x<-50$ μm, and the other is effective pulse compression working point with $\Delta x=0$ μm nearby, where high peak

power and effective pulse width compression of 1st Stokes laser can be achieved. For these two working points, output features of synchronously pumped diamond Raman lasers are investigated with respective to Raman crystal length, pumping power, OC reflectivity and pumping pulse width.

For both 532 nm and 1064 nm pumping, high Raman conversion efficiency can be achieved for $\Delta x < -50$ μm, diamond crystal length of 5 mm, pumping pulse width of 10 ps and pumping power of 2 W. Higher efficiency can be obtained with longer Raman crystal, longer pumping pulse width and higher pumping power.

For 532 nm pumping, effective pulse width compression can be realized for $\Delta x = 0$ nearby, diamond crystal length of 10 mm, pumping pulse width of 15 ps, $R > 90\%$ and pumping power of 2 W. Shorter pulse width and higher peak power of 1st Stokes laser can be achieved with longer Raman crystal, shorter pumping pulse width and higher pumping power.

Author contributions Shuanghong Ding: Conceptualization, Methodology, Software, Writing. Xinxin Huang: Data curation, Visualization. Qiaoshuang Zou: Investigation.

Declarations

Competing interests The authors declare no competing interests.

References

1. D. Spence, E. Granados, R. Mildren, Opt. Lett. **35**, 556 (2010)
2. R. Mildren, A. Sabella, Opt. Lett. **34**, 2811 (2009)
3. A. Sabella, J. Piper, R. Mildren, Opt. Lett. **35**, 3874 (2010)
4. A. Sabella, J. Piper, R. Mildren, Opt. Express **19**, 23554 (2011)
5. M. Jelínek, O. Kitzler, H. Jelínková, Laser Phys. Lett. **9**, 35 (2012)
6. A. Sabella, J. Piper, R. Mildren, Opt. Lett. **39**, 4037 (2014)
7. E. Granados, D. Spence, Opt. Express **18**, 20422 (2010)
8. S. Ding, H. Li, X. Che, S. Peng, Opt. Express **28**, 35251 (2020)
9. H. Li, S. Peng, X. Huang, S. Ding, Appl. Phys. B **128**, 101 (2022)
10. A. Penzkofer, A. Laubereau, W. Kaiser, Prog. Quant. Electron. **6**, 55 (1979)
11. E. Granados, H. Pask, D. Spence, Opt. Express **17**, 569 (2009)